9-6-91
E6430

NASA Technical Memorandum 105149
AIAA-91-2228

Preliminary Performance and Life Evaluations of a 2-kW Arcjet

W. Earl Morren and Francis M. Curran
Lewis Research Center
Cleveland, Ohio

NASA

Preliminary Performance and Life Evaluations of a 2-kW Arcjet

W. Earl Morren* and Francis M. Curran*
National Aeronautics and Space Administration
Lewis Research Center
Cleveland, Ohio 44135

ABSTRACT

The first results of a program to expand the operational envelope of low-power arcjets to higher specific impulse and power levels are presented. The performance of a kW-class laboratory model arcjet thruster was characterized at three mass flow rates of a 2:1 mixture of hydrogen and nitrogen at power levels ranging from 1.0 to 2.0 kW. This same thruster was then operated for a total of 300 h at a specific impulse and power level of 550 s and 2.0 kW , respectively, in three continuous 100-h sessions. Thruster operation during the three test segments was stable, and no measurable performance degradation was observed during the test series. Substantial cathode erosion was observed during an inspection following the second 100-h test segment. Most notable was the migration of material from the center of the cathode tip to a ring around a large crater. The anode sustained no significant damage during the endurance test segments. Some difficulty was encountered during start-up after disassembly and inspection following the second 100-h test segment, which caused constrictor erosion. This resulted in a reduced flow restriction and arc chamber pressure, which in turn caused a reduction in the arc impedance.

INTRODUCTION

Demands for high-performance auxiliary propulsion systems on commercial communications satellites have driven an intense effort toward the development of kilowatt-class arcjet propulsion systems. This is because the performance advantages that these systems offer over existing resistojet and chemical systems lead to significant reductions in north-south stationkeeping propellant requirements.

During the 1980's arcjet system development has focussed on meeting the technology goals necessary to bring these systems to flight readiness. Stable and reliable operation on hydrazine decomposition products at specific impulse levels of 450 to 500 s has been demonstrated[1-4]. Pulse width-modulated power processing units incorporating high-voltage pulsed starting circuits have been tested[5-7]. Extended, cyclic endurance tests on both laboratory[8] and flight-type[7] arcjet systems have been completed. Other studies have focussed on the impacts of arcjet system integration. Electron number densities and temperatures have been measured in both the near- and far-field arcjet plume using Langmuir probes[9-12]. The results of these plume surveys have been used to model the effects of the slightly-ionized plumes on communications signals[13,14]. Testing of a flight-type arcjet system on a spacecraft simulator directed toward the documentation of spacecraft/arcjet system interactions has been completed[15]. The culmination of these efforts has been the selection of an arcjet system to provide stationkeeping on a new generation of commercial spacecraft[16].

Future specific impulse requirements are expected to increase, as are the limits of power available to spacecraft propulsion systems. Anticipating these requirements, a program was initiated to expand the envelope of low-power arcjet operation beyond the current state-of-the-art (approximately 530 s mission-average at 1.6 kW into the thruster using hydrazine propellant) to 600 s and thruster power levels of 2 to 5 kW. The purpose of this paper is to present the results of the first step toward that goal.

Arcjet specific impulse is closely tied to the energy input per unit mass of propellant expelled. Increasing the state-of-the-art specific impulse requires increasing the ratio of input electric power to propellant mass flow rate (referred to herein as specific power) and/or reducing the various losses inherent in arcjet operation. Thermal, frozen flow (i.e., energy not recovered as thrust), and nozzle losses are dominate factors in arcjet efficiency. An investigation into means of reducing thermal losses is under way[17] and an earlier effort showed that increasing nozzle expansion ratio increased thruster efficiency[18]. Additional near-term programs are attempting to reduce frozen flow losses. This effort seeks to enhance specific impulse by increasing the specific power.

The first step toward expanding the operating envelope beyond the current state-of-the-art was to identify the life-limiting issues in the current thruster technology at conditions beyond those typical of low-power arcjets. To this end a modular laboratory model arcjet thruster was run for a total of 300 h in three continuous 100-h test segments at constant specific impulse and power levels of 550 s and 2.0 kW, respectively, on a mixture of hydrogen and nitrogen simulating hydrazine decomposition products. Performance was measured at propellant mass flow rates ranging from 3.0×10^{-5} to 5.0×10^{-5} kg/s and thruster input power levels ranging from 1.0 to 2.0 kW. The accompanying text describes the test thruster, facilities, and procedure. Also included are the results of four performance characterizations conducted over the life of the lifetest thruster, as well as the details of one interim and one post-test disassembly and inspection.

APPARATUS AND PROCEDURE

Thruster. Figure 1 shows a schematic diagram of the lifetest thruster, which was a modular laboratory design. The cathode was a 3.18 mm diameter 2% thoriated tungsten rod with a cone of 30° half-angle ground on one end. The anode, also fabricated from 2% thoriated tungsten rod, incorporated a nozzle with a conical convergent section with a 30° half-angle, a 0.55 mm diameter by 0.25 mm long cylindrical constrictor, and a conical divergent section with a 20° half-angle. The expansion area ratio was 214. Figure 2 shows an exploded view of the cathode tip/anode constrictor region. The arc gap (the minimum axial distance between the cathode tip and the anode) was set to 0.58 mm. This was accomplished by inserting the cathode into the thruster until it met the anode, then withdrawing it by the desired gap setting. The electrodes were contained in a housing fabricated from titaniated-zirconiated-molybdenum (TZM). The anode housing had a 0.25 mm thick layer of molybdenum powder plasma-sprayed onto the exterior surface to enhance its emittance.

The joint between the anode and the housing was a tapered interference fit 6.35 mm in length with a 5° half-angle and a minor diameter of 13.7 mm. This joint was lapped during thruster assembly to aid thermal conduction from the anode to the housing and to minimize gas leakage. A TZM injector disk was located immediately behind the anode. Two 0.38 mm diameter holes in the disk injected the propellant into the arc chamber, the small plenum surrounding the cathode tip, so as to set up a vortex flow field. This was

done because a vortex flow has been shown to improve starting and steady state stability. However, no systematic study has yet been conducted to evaluate the effects of vortex strength on arcjet stability.

Behind the injector disk was a boron nitride insulator (the front insulator in figure 1). The front insulator served to provide electrical isolation of the cathode from the anode-potential housing; to force the gas flow through several axial channels located next to the housing wall; and to transmit the compressive force imparted by the spring, located in the rear half of the thruster, to the front insulator/injector and injector/anode joints. The compressive forces on the joints around the injector were required to assure that the propellant flowed through the injector ports and not around the injector. Flowing the propellant next to the anode housing wall provided some regenerative cooling of the anode region.

The upstream end of the thruster was contained in the boron nitride rear insulator. The propellant and cathode feedthrough fittings were commercially-available compression fittings modified to mate with flats machined into the rear insulator. These joints were sealed with gaskets made from 0.25 mm thick graphite foil. An inconel spring located within the rear insulator provided the compressive force necessary to prevent leakage around the injector disk while allowing for thermal expansion of the internal thruster components. A boron nitride plunger transmitted the compressive force to the front insulator which in turn pushed the injector disk against the rear of the anode. Graphite foil gaskets between the front insulator, the injector disk, and the anode prevented gas from blowing by the injector disk. Note that it was necessary for the front insulator to slide freely over the cathode within the anode housing for it to effectively transmit the springs force to the injector joints. The rear insulator was clamped to the anode housing by two 1.6 mm thick molybdenum flanges and four

number 10 stainless steel bolts. Graphite foil gaskets sealed this joint. Figure 3 shows a photograph of this design prior to assembly.

During operation, propellant was fed to the thruster propellant feedthrough. The gas flowed over the spring, through several axial channels in the boron nitride ram and into a plenum between the front and rear insulators. From there the gas flowed through sixteen axial channels, approximately 0.5 mm square in cross-section, cut into the outer surface of the front insulator. This placed the gas in direct contact with the housing and provided some regenerative cooling of the forward end of the thruster. The gas then flowed through two 0.381 mm diameter holes in the injector disk and into a small plenum around the cathode tip (the arc chamber). The gas was injected into the arc chamber so as to set up a vortical flow. The gas then passed through the constrictor where it is heated by the arc and is accelerated in the nozzle, producing thrust.

Propellant. The propellant used was a mixture of hydrogen and nitrogen at a mixture ratio of 2:1 by volume, simulating hydrazine decomposition products. The pure (99.99% minimum) gases were stored in high-pressure bottles, then metered separately and mixed upstream of the thruster. The mixture entered the thruster at room temperature.

Power Processing. Power was supplied to the thruster from a pulse width-modulated power processing unit (PPU) with high-speed current regulation. The PPU was capable of delivering up to 130 Vdc and 50 A to the thruster. Starting was facilitated by a built-in, high-voltage circuit capable of providing a 4 kV pulse every second until breakdown occurred. Starting current surge protection kept the PPU from delivering maximum current until the arc had sufficient time to blow through the constrictor, seating in the nozzle divergent section. Earlier efforts to start without this surge protection often

resulted in constrictor damage due to momentary spot attachment in high-pressure regions upstream of the constrictor at high current levels. Further details of this PPU have been detailed elsewhere[19].

Test Facilities. Two test facilities were used to carry out these experiments. All performance characterizations were conducted in a cylindrical vacuum tank measuring 1.5 m in diameter by 4.5 m long. This tank was equipped with four 0.8 m diameter oil diffusion pumps backed by a lobe-type blower and two rotary piston roughing pumps. The test cell background pressure was below 0.1 Pa for all performance tests. During operation in this facility the thruster was mounted on a thrust stand in a horizontal orientation, on the axis of the vacuum tank. Figure 4 shows a photograph of an arcjet operating in the performance test facility.

Figure 5 shows a photograph of an arcjet mounted in the endurance test facility, a cylindrical vacuum chamber 0.5 m in diameter by 0.6 m high. This test cell was equipped with a rotary piston roughing pump capable of maintaining test cell pressures of approximately 100 Pa during all endurance tests. During operation in this facility the thruster was mounted in a vertical axis orientation and fired directly into the inlet of the pumping system.

Operational parameters monitored during all tests included arc voltage and current, hydrogen and nitrogen mass flow rates, propellant feed pressure, and temperature of the exterior of the anode housing. Thrust was measured only during performance characterization. All data were monitored, reduced, displayed, and stored using a microcomputer-based data acquisition and control system (DACS). Data were stored every 30 seconds throughout the endurance tests. The performance and endurance test data acquisition programs were written using a graphically-driven software system which facilitated real-time reduction of all

transducer signals into engineering units, as well as calculation of several derived parameters. These data were then displayed in digital and graphical forms on the computer screen at a sampling rate of about 1.5 Hz. This system also controlled automatic shutdown of the thruster power and propellant flow in the event any monitored parameters deviated from designated ranges. This permitted unattended operation of the thruster.

The arc voltage was measured at the power leads connecting the PPU to the test facilities. The arc current was measured using a shunt in series with the thruster. The current signal was processed using a low-pass analog filter with a time constant of about 0.5 s. The filter was necessary to obtain a dc-level signal because the current had about 5% ripple at 20 kHz. Both voltage and current signals were then fed to the DACS through isolation amplifiers. The DACS responses to the voltage and current inputs were calibrated by removing the PPU from the electrical circuit, then applying reference voltages and currents to the signal conditioning system from a laboratory dc power supply.

Propellant mass flow rates were measured using commercially-available thermal conductivity-type mass flow meters with operating ranges of 0 to 10 SLPM. These units maintained steady propellant mass flow rates by using flow sensor feedback to control integral solenoid-operated flow control valves. The mass flow controllers were calibrated in-situ at each of the test facilities using a volumetric standard, as is common practice in the flow measurement industry. The individual gases were flowed through the respective mass flow controllers, then into a cylinder of known volume. The pressure and temperature in the cylinder were measured before and after flowing gas into the cylinder, and the length of time gas flowed into the cylinder was recorded. The mass added to the cylinder was then calculated assuming ideal gas behavior. This

standard had an estimated uncertainty of about 1%, with typical repeatabilities better than 1%.

Thrust was measured by a calibrated displacement-type thrust stand designed and fabricated at the NASA Lewis Research Center. This unit was equipped with numerous water cooling passages throughout the structure to minimize thermal drift due to component expansion during thruster operation. Thermal drift was observed to be less than 1% of the nominal thrust level during all tests, and was found to be always in the direction of decreasing thrust. Therefore, all thrust measurements were corrected by recalibrating the thrust stand while hot, making any residual thrust measurement error conservative. Additional details of this thrust measurement system are available elsewhere[20].

The propellant feed pressure to the thruster was monitored using a strain-gage type pressure transducer with a range of 0 to 1.4 MPa. It is important to note that the measured pressure is that of the propellant upstream of the injector disk, which was estimated to be substantially higher than the arc chamber pressure. Furthermore, the pressure drop across the injector disk was a function of thruster operating conditions. Nonetheless, the feed pressure was useful as an indication of the integrity of the flow path and pressure vessel during operation.

The temperature of the anode housing surface (see Fig. 1 for location) was measured using a two-color optical pyrometer with a range of 700 to 1400°C. This device used the ratio of the energy emitted at two wavelengths (both in the vicinity of 1 μm) to calculate the target surface temperature. The output reading was not sensitive to the absolute value of the emittance, but to the slope of the variation of emittance with wavelength.

Test Procedure. The objective of this test series was to identify the life-limiting issues of arcjet thruster operation at a specific impulse and power level of 550 s and 2.0 kW, respectively. The approach was to conduct a series of 100-h endurance tests with intermittent thruster performance characterizations and physical examinations. Figure 6 shows the test chronology time line. Prior to assembly the electrode masses were recorded. The constrictor dimensions were determined by making a mold of the constrictor region using a vinyl-polysiloxane analogue (dental putty), then inspecting the mold under a microscope equipped with a three-axis translation stage assembly. The length of the anode protruding from the end of the anode housing was also recorded.

Immediately following assembly the thruster was installed in the endurance test facility for a 20-h burn-in period. Laboratory experience has demonstrated the tendency with a new cathode for the arc voltage to increase substantially over the first 20 to 30 h of operation at constant mass flow rate and current. The purpose of the burn-in period was to bring the electrode to a condition more representative of steady state prior to the initial performance characterization of the thruster. During most of this phase of testing the thruster was operated at a flow rate of 5.0×10^{-5} kg/s and a power level of 1.5 W. The last several hours of burn-in included operation at 1.75 and 2.0 kW, also at a mass flow rate of 5.0×10^{-5} kg/s.

Following burn-in, the thruster was installed on the thrust stand to characterize thruster performance. This was done to provide a baseline for interim and post-test comparison, and to aid in selecting the mass flow rate for the endurance test. As shown in Table I, performance was measured at each of three mass flow rates (3.0×10^{-5}, 4.0×10^{-5}, and 5.0×10^{-5} kg/s) at up to 5 power levels (1.0, 1.25, 1.5, 1.75, and 2.0 kW). The boundaries of the operating

5

envelope were defined by a PPU output voltage limit of 130 V and an anode housing temperature limit of 1400°C.

Following the initial performance characterization, the thruster was installed in the endurance test facility and run for 100 h at a power level and specific impulse of 2.0 kW and 550 s (nominal), respectively. Due to the current-regulating nature of the power supply, it was necessary to reduce the current setpoint occasionally during the endurance tests to maintain a constant 2.0 kW as the arc impedance increased with time. At the end of the first 100 h, the thruster was reinstalled on the thrust stand and characterized to document any performance changes. After the 100-h performance check the thruster was moved back to the endurance test facility where it was run another 100 h at 2.0 kW and 550 s. Upon completion of the second 100-h test segment, the thruster performance was checked, following which it was disassembled for inspection.

The third 100-h test segment was preceded by a performance characterization. For reasons which will be discussed later, graphite foil gaskets were not used in the injector disk seals during this test segment. An anomaly during the first restart resulted in some constrictor damage. This necessitated another disassembly and inspection, during which the surfaces of the injector disk were cleaned and the inconel spring was stretched to increase the preload on the injector seals. The performance characterization was then completed and a third 100-h test segment was conducted.

After completing a total of 300 h at the nominal operating conditions the thruster was disassembled for inspection a second time. No performance characterization was performed prior to this inspection. The thruster was reassembled after the electrodes were examined so that the performance could be measured. However, starting difficulties were encountered, and the performance tests

were cancelled. The thruster was disassembled a final time, after which the electrodes were sectioned for metalographic analyses.

RESULTS AND DISCUSSION

Performance Characterizations. Table II summarizes performance data acquired during this test series. Figure 7 shows the measured specific impulse versus specific power (i.e., the ratio of electric power to mass flow rate) for the test thruster following the 20-h burn-in period. These data (labelled "0 h" in Table II) provided a baseline against which to measure any changes in thruster performance during the course of the endurance test series. This test also showed that the mass flow rate necessary to obtain the specified endurance test condition of 550 s at a power level of 2.0 kW was 5.0×10^{-5} kg/s. Note that the specific impulse at a given specific power was dependent upon mass flow rate. This has been observed previously in lower-power arcjets[21]. To date there are insufficient data to understand this phenomenon. Also shown in Fig. 7 are performance data obtained in previous arcjet tests[2,21,22]. Agreement with the data of the current effort is generally good. The Ref. 2 data were acquired at two different test facilities. The uppermost point was measured in an industrial test cell at a mass flow rate and power level of 4.4×10^{-5} kg/s and 2.0 kW, respectively, using hydrazine propellant. The other Ref. 2 datum was measured at a government facility at 2.8×10^{-5} kg/s and 1.0 kW on a 2:1 hydrogen-nitrogen mixture. Although the Ref. 21 data were obtained at a variety of mass flow rates, they were all measured at specific power levels below 15 MJ/kg. At that point the effects of mass flow rate variations on specific impulse began to disappear. The Ref. 22 data were measured at LeRC on a hydrogen-nitrogen mixture at a mass flow rate of about 4.1×10^{-5} kg/s. Both points are within approximately 3% of the 4.0×10^{-5} kg/s data acquired during the current effort. Other performance data at

6

comparable conditions indicate good agreement as well[18,23].

Figure 8 shows the results of the performance characterizations conducted during the test series at a flow rate of 5.0×10^{-5} kg/s. Figures 9 and 10 show the corresponding performance at flow rates of 4.0×10^{-5} kg/s and 3.0×10^{-5} kg/s, respectively. No degradation of thruster performance is indicated at any of the operating conditions tested. This is particularly interesting in consideration of an anomaly experienced during the first restart of the thruster after the 200-h disassembly and inspection. An apparent leak around the injector disk resulted in substantial erosion of the constrictor. This caused the arc chamber pressure at a given mass flow rate and power level to decrease, which lead to a decrease in arc impedance at all operating conditions. Further details of this anomaly will be given in a later section. The most important result was that thruster performance and stability were not impacted by the constrictor damage.

Endurance Tests. Figures 11, 12, and 13 show the arc voltage, propellant feed pressure, and anode housing temperature, respectively, at 30-second intervals over the endurance test series. As discussed earlier, the test plan called for a series of 100-h continuous endurance test segments with intermittent performance characterizations and physical examinations. Three unscheduled shutdowns also occurred, one during each of the 100-h test segments. The first occurred about 20 h into the first test, caused by interruption of the two-color pyrometer signal to the DACS. This violated the lower shut down setpoint for this parameter, which in turn shut down the propellant flow and PPU. The test was restarted after about one hour without difficulty. None of the thruster operating parameters was out of its specified range prior to this shutdown, although a declining feed pressure trace (see Fig. 12) was causing some concern. This will be discussed in greater detail

later in this section. The second and third unintended shutdowns occurred after approximately 173 and 230 h of thruster operation, respectively. In each case a facility interlock for the thruster power supply was violated, causing a loss of power to the PPU. The test was restarted within about 45 minutes of the second shutdown, and immediately following the third shutdown. Each time the thruster restarted without difficulty. Neither of these shutdowns was caused by any irregularity in thruster operation.

The arc voltage increased during the first 200 h of operation at an average rate of 35 mV/h. As shown in Fig. 11, the thruster experienced periods of increasing and decreasing voltage, although all voltage values fall within a band of ± 2.5 V from the nominal value at that point in the test. This represents a variation of about 2.2% of the average arc voltage measured during the first two 100-h test segments. Arc voltage fluctuations of this magnitude have been observed in previous endurance tests[8,23]. During the third 100-h test the voltage rose at a substantially lower rate. This test segment was also relatively free of the voltage excursions typical of the first two endurance tests. However, the voltage during this test was several volts lower than during the first two test segment due to the constrictor damage sustained prior to this test segment.

During most of the endurance tests the propellant feed pressure remained steady. There were two instances, however, when the feed pressure declined gradually over periods of about 20 h and 50 h during the early portions of the first and second test segments, respectively (see Fig. 12). Either of these trends could have indicated a leak from the thruster pressure vessel, an increase in constrictor diameter, or a leak past the injector disk into the arc chamber. The most serious leak would be from the thruster pressure vessel because this would have been a failure resulting in the loss of performance and, perhaps, the failure of

7

the thruster. Concurrent symptoms of a pressure vessel leak would have been declining arc voltage and increasing anode housing temperature (due to an increase in the effective specific power). The symptoms of an increase in constrictor diameter are similar to those of a leaking pressure vessel: concurrent decreases in arc voltage and feed pressure. Leakage past either of the injector disk seals would have allowed propellant to bypass the two injector ports. This would result in a reduction in feed pressure, accompanied by irregular arc voltage excursions, although no general trend toward decreasing arc voltage would be expected. The arc voltage excursions could be due to rapid movement of the arc seat about the cathode tip in the absence of sufficient vortex stabilization in the arc chamber.

During the first 20 h of the first 100-h test segment the feed pressure gradually decreased from its original value of 680 kPa to about 640 kPa. Over the same period the anode housing temperature increased by about 30°C to 1330°C and the arc voltage remained steady at 109 V. Following the first unintended shutdown, the feed pressure and the anode housing temperature returned to their original values of 680 kPa and 1330°C, respectively. At that time it was speculated that the front insulator might have been sticking to the cathode or anode housing prior to the shutdown. This would have defeated the spring in the rear of the thruster, allowing the compressive force on the injector seals to be relieved, and resulting in leakage past the injector. The thermal cycle associated with the shutdown could then have freed the insulator, allowing the thruster to return to its original condition. No significant pressure variations were encountered for the remainder of the first 100-h test segment.

During the first half of the second 100-h test. The feed pressure gradually decreased from an initial value of approximately 680 kPa to a minimum of 630 kPa. Between 100 and 135 h the voltage fell from an initial value of 112 V to a minimum of about 110 V and the anode housing temperature rose to a maximum of nearly 1400°C. These trends suggested the possibility of a leak from the thruster pressure vessel or constrictor erosion. However, the voltage began a strong recovery and the anode housing temperature fell sharply at about 135 h, while the feed pressure was still falling. At about 150 h the feed pressure and arc voltage increased in a step change to 680 kPa and 115 V, respectively. The arc voltage, feed pressure, and anode housing temperature were relatively steady during the remainder of the second test segment.

Thruster Inspections. As shown in Fig. 6, the thruster was disassembled for inspection following the second 100-h endurance test. The overall thruster length was measured prior to disassembly. This was necessary for determination of the arc gap later in the disassembly. The overall length was found to have increased by about 0.56 mm. The length of portion of the anode protruding from the anode housing was also measured. The anode had moved within the tapered seat in the anode housing as indicated by a 0.56 mm increase in the length of the protruding portion. Because the cathode was tied rigidly to the rear of the thruster, movement of the anode within the housing would result in an increase in the arc gap. The movement of the anode within the anode housing could have contributed to the pressure variations observed during the first two test segments by allowing propellant to leak past the tapered seal or by relieving some of the compressive force on the injector seals.

The arc gap was determined by measuring the overall thruster length with the cathode pushed in until it met the anode, then subtracting this length from the overall length measured previously. The arc gap was found to have increased by 0.013 mm, which was about 0.55 mm

less than was expected based on the increase in the length of the anode protruding from the housing.

The discrepancy between the measured arc gap and the forward movement of the anode within the housing was explained when the cathode was removed from the thruster for inspection. The tip of the cathode had formed a crater nearly 1.3 mm in diameter with a bulged rim (see Fig. 14). The material on this rim lay outside the original conical envelope by an amount approximately equal to the distance moved by the anode. The axial distance from the original tip location to the crater rim was approximately 0.58 mm. Figure 15 shows a sketch of the cathode tip with the original conical tip shape superimposed for comparison. Of particular interest was the migration of material from the center of the cathode tip to a region outside the original conical shape of the cathode tip. This could have resulted in shorting of the cathode to the anode had the anode not moved forward within the housing. The measured cathode mass loss was approximately 2×10^{-6} kg.

Figure 5a of reference 24 shows a cross section of a 2% thoriated tungsten cathode tip operated for 9 h in three thermal cycles at a current of 11 A. The overall diameter of the crater in that cathode tip was only about 0.5 mm (versus 1.3 mm for the current specimen). However, the movement of material to a region outside the original conical shape of the tip bears a striking resemblance to the current test results. This suggests that the observed cathode erosion was driven by some phenomenon which was not time dependent.

The tip of another cathode run for a total of 1000 h and 500 thermal cycles at a constant current of 11 A displayed a distinctly different type of erosion[8]. The results of that test showed a crater slightly smaller than that of the current test, but the rim of the cathode was not bulged. Instead, the crater rim had several axial cracks. Differences in the operating histories of these two cathodes include a lower arc current and anode temperature (by at least 400°C), and substantially greater number of starts on this cathode than that of the current work.

Inspection of the graphite gasket between the insulator and the injector disk revealed some holes, although the actual sealing surface was intact. However, the gasket between the injector disk and the anode had been completely consumed, leaving no visible trace. This had been observed in a previous life test conducted by the author during which the anode had operated at temperatures some 500°C higher than in the current tests. As was discussed earlier, some degradation of the injector sealing was believed to be responsible for the pressure fluctuations observed during the first two 100-h endurance tests. The lack of any remnants of the forward graphite foil gasket confirmed those suspicions. Of particular interest was the fact that the thruster resumed stable operation after each of the pressure excursions, suggesting that the graphite foil gaskets were unnecessary components.

The anode was not removed from the housing at this time to avoid disturbing the tapered seal between these two components. However, examination of the constrictor exit under a microscope revealed no substantial degradation. Some metal deposits lined the nozzle wall near the constrictor exit, but the constrictor was still circular and its diameter had increased by only 0.015 mm (to 0.57 mm).

The thruster was reassembled and its performance was characterized in preparation for a third 100-h test segment. The only deviation from previous thruster assembly procedures was the deletion of graphite gaskets around the injector; this in an effort to return the thruster to a condition as close as possible to that prior to the disassembly. The arc gap was set to 0.60

mm (the same as at the end of the second 100-h test). The first several attempts to restart the thruster resulted in short durations of low mode operation (where the arc attaches to the anode upstream of the constrictor in a high-pressure). After the more benign high mode operating condition (characterized by diffuse, higher-voltage attachment in the divergent section of the nozzle) was finally achieved, it was apparent that the thruster was not operating properly. Arc voltage was unsteady and the measured specific impulse was substantially lower than had been measured immediately prior to the disassembly and inspection. The performance test was terminated and the thruster was disassembled for inspection. Substantial constrictor erosion had occurred during the several low-mode starting attempts. A large chunk of material had been removed from one side, leaving the constrictor with an egg-shaped cross section with a flow area approximately 25% larger than before this test. The cause of the errant operation was believed to have been caused by inadequate sealing at the front insulator/injector and injector/anode joints. This could have resulted in sufficient injector blow-by to cause the vortex flow within the arc chamber to be disrupted. This, in turn, could have allowed the arc to seat in the low mode and resulted in unstable operation once the arc had seated in the high mode. The seating surfaces of the injector disk were cleaned to assure proper mating with the anode and front insulator surfaces, and the spring was stretched to increase the compressive force on the insulator/injector and injector/anode joints. No graphite foil gaskets were installed around the injector. The next start-up was typical of a properly-operating arcjet, with a quick transition to high-mode operation and a steady voltage trace thereafter.

At the completion of the third 100-h test segment the thruster was disassembled for another inspection. No additional anode movement had occurred. Some additional cathode erosion had occurred,

however. Figure 16 shows a photograph of the cathode tip. Figure 17 shows a sketch of the cathode tip profile with the as-machined shape superimposed for comparison. The shape of the tip is similar to that seen during the previous inspection (see figure 14), although the diameter of the crater had increased by 0.06 mm to 1.35 mm. The lip of the crater had recessed 0.20 mm (nominally) from its position after the second 100-h test, for a total tip recession of 0.86 mm from the as-machined tip location. The cathode mass was approximately 1×10^{-6} kg lower than that measured after the second 100-h test segment, for a total cathode mass loss of about 3×10^{-6} kg over the three test segments.

An attempt was made to recharacterize the thruster performance following the second disassembly and inspection. However, difficulty was encountered during the first start, much the same as was experienced after the first disassembly and inspection. It was decided not to proceed with this performance characterization, perhaps risking destruction of information about the electrodes.

The starting difficulties encountered after each of the disassemblies highlighted the sensitivity of the thruster design to the precision of the fits between the front insulator, injector, and anode. The graphite foil gaskets typically used in these seals tend to fill any voids between the parts. The absence of these gaskets, however, can allow sufficient injector blow-by to weaken the vortex flow field within the arc chamber, leading to unstable operation. The fact that the test thruster operated successfully without the gaskets was fortuitous. It is important to note that these gaskets were necessitated by design features specific to the test thruster; flight-type arcjet systems do not employ such gaskets. Future modular arcjet designs intended for operation at conditions similar to these should avoid the use of graphite gaskets.

10

The thruster was disassembled a final time and the anode and cathode tip were sectioned for metalographic analyses. Figure 18 and 19 show two views of the cathode tip. In Fig. 18 the crater rim does not appear to be as dramatically bulged as in Fig. 16 (taken after 300 h of operation, but before the last unsuccessful attempts to restart the thruster). Figure 19 does not display the textured surface within the crater, as does Fig. 16, nor is any distinct molten pool, where arc attachment would have occurred, apparent. Only a few minutes of unstable operation occurred between the conditions identified in Fig. 16 and Figs. 18 and 19. Apparently the arc attachment point was moving about on the surface of the cathode tip, leaving a trail of molten material in its path which solidified as the arc moved on.

Figure 20 shows a scanning electron microscope (SEM) photograph of the constrictor exit at the conclusion of these tests. As was discussed earlier, most of the constrictor erosion occurred during the few minutes of low-mode operation experienced following the 200-h and 300-h disassemblies. The cracks traversing the constrictor have been observed in previous tests[8,25]. Although the degradation of the constrictor was extensive, it is important to note that no reduction in thruster performance was measured.

The electrodes were sectioned and prepared for analyses of the grain structures and compositions in the regions of arc attachment. Figure 21 shows a photograph of the grain structure of the cathode tip. Three distinct grain structures are apparent. Much of the cathode exhibited the fine, axially-oriented grain structure characteristic of wrought tungsten. Close to the tip the grains were larger, indicating the tungsten cathode material recrystalized during the test series. This recrystalized zone extended from the tip along the cathode axis for a distance of nearly 6.4 mm and was approximately one-third the cathode

diameter over most of this length. The surface of the crater was lined by a few very large crystals, evidence that this entire surface had been molten at some time during the test series.

Figure 22 shows a photograph of the grain structure near the cathode tip at a higher magnification. From this it is clear that most of the material lying outside the original conical shape of the tip was molten at some time during the test. Some of the grains outside the molten region also lie outside the original conical envelope. The deformation of the solid tungsten could not be studied by conventional structural analysis techniques due to the inelastic behavior of tungsten at the temperatures encountered.

Figure 23 shows a photograph of the grain structure of the anode. Note that the extent of recrystalization was not azimuthally uniform, indicating that the temperature of this component was not axisymmetric. The reason for this asymmetry could not be determined from the available data.

CONCLUSIONS

The test thruster successfully completed three 100-h endurance test segments operating at specific impulse and power levels of 550 s and 2.0 kW, respectively. No degradation in thruster performance was measured during the test series. Thruster operation was stable during all test segments, although the propellant feed pressure did fall on two occasions during the first two test segments. Each time the feed pressure recovered and thruster operation returned to the nominal conditions.

Degradation of the graphite foil gaskets used in the injector disk seals was believed to have contributed the feed pressure excursions noted above. Future efforts to operate modular thrusters for extended times at conditions similar to these should avoid the use of graphite foil gaskets in high-temperature regions of the thruster. Movement of the anode within

the anode housing could also have played a role, particularly during the second such incident when symptoms suggested a leak from the pressure vessel.

Erosion of the cathode tip was substantial. The cathode lost a total of approximately 3×10^{-6} kg and the original conical tip receded 0.78 mm along the axis to form a crater 1.35 mm in diameter, and surrounded by a bulging rim. This bulge could have caused the electrodes to short had the anode not moved forward within the anode housing during operation. A combination of flowing molten tungsten and yielding of the solid tungsten under the influence of thermal stresses are believed to have caused the cathode tip bulging. Further testing should be done to evaluate the effects of cathode reconfiguration, arc chamber pressure, arc current, and operating cycle duration on cathode life.

Anode erosion at the steady state conditions tested did not present any issue. The only degradation of the anode occurred during a brief session of low-mode operation, when a large chunk of tungsten was removed from the constrictor. This incident underscored the importance of stable operation to anode life. No degradation of performance was measured after this incident, and thruster operation was stable during the 100-h test which followed.

REFERENCES

1. Hardy, T. L., and Curran, F. M.,"Low Power dc Arcjet Operation with Hydrogen/Nitrogen/Ammonia Mixtures," AIAA-87-1948, June 1987.

2. Knowles, S. C., Smith, W. W., Curran, F. M., and Haag, T. W.,"Performance Characterization of a Low Power Hydrazine Arcjet," AIAA-87-1057, May 1987.

3. Knowles, S. C., et al,"Performance Characterization of a Low Power Hydrazine Arcjet," NASA CR-182107, August 1987.

4. Knowles, S. C., and Smith, W. W.,"Arcjet Thruster Research and Technology," Rocket Research Company, Redmond, WA, NASA CR-182276 (to be published).

5. Gruber, R.P.,"Power Electronics for a 1-kW Arcjet Thruster," AIAA-86-1507, June 1986.

6. Sarmiento, C. S., and Gruber, R. P.,"Low Power Arcjet Thruster Pulse Ignition," AIAA-87-1951, July 1987.

7. Knowles, S. K., Yano, S. E., and Aadland, R. S.,"Qualification and Lifetesting of a Flight Design Hydrazine Arcjet System," AIAA-90-2576, July 1990.

8. Curran, F. M., and Haag, T. W.,"An Extended Life and Performance Test of a Low-Power Arcjet," AIAA-88-3106, July 1988.

9. Zana, L. M.,"Langmuir Probe Surveys of an Arcjet Exhaust," AIAA-87-1950, July 1987.

10. Carney, L. M.,"An Experimental Investigation of an Arcjet Thruster Exhaust Using Langmuir Probes," Master's Thesis, University of Toledo, NASA TM-100258, December 1988.

11. Carney, L. M., and Sankovic, J. M.,"The Effects of Arcjet Operating Condition and Constrictor Geometry on the Plasma Plume," AIAA-89-2723, July 1989.

12. Sankovic, J. M.,"Investigation of the Arcjet Plume Near Field Using Electrostatic Probes," presented at the 1990 JANNAF Propulsion

Meeting, Anaheim, CA, October 1990 (NASA TM-103638).

13. Carney, L. M.,"Evaluation of the Communications Impact of a Low Power Arcjet Thruster," AIAA-88-3105, July 1988.

14. Ling, H., et al,"Reflector Performance Degradation due to an Arcjet Plume," presented at the 1989 Antenna Applications Symposium," Monticello, IL, September 1989.

15. Zafran, S.,"Arcjet System Integration Development Program," TRW, Inc., Redondo Beach, CA, NASA CR-1187147 (to be published).

16. Smith, R. D., Roberts, C. R., Davies, K., and Vaz, J.,"Development and Demonstration of a 1.8 kW Hydrazine Arcjet Thruster," AIAA-90-2547, July 1990.

17. Sankovic, J. M., and Curran, F. M.,"Arcjet Thermal Characteristics,"AIAA-91-, June 1991.

18. Curran, F. M., Sarmiento, C. J., Birkner, B. W., and Kwasny, J.,"Arcjet Nozzle Area Ratio Effects," presented at the 1990 JANNAF Propulsion Meeting, Anaheim, CA, October 1990 (NASA TM-104477).

19. Gruber, R. P., Gott, R. W., and Haag, T. W.,"5-kW Arcjet Power Electronics," AIAA-89-2725, July 1989.

20. Haag, T. W., and Curran, F. M.,"Arcjet Starting Reliability: A Multistart Test on Hydrogen/Nitrogen Mixtures," AIAA-87-1061, May 1987.

21. Curran, F. M., and Sarmiento, C. J.,"Low Power Arcjet

Performance," AIAA-90-2578, July 1990.

22. Curran, F. M., Sovie, A. J., and Haag, T. W.,"Arcjet Nozzle Design Impacts," NASA TM-102050, May 1989.

23. Curran, F. M., Hardy, T. L., and Haag, T. W.,"A Low-Power Arcjet Cyclic Lifetest," NASA TM-100233, December 1987.

24. Curran, F. M., Haag, T. W., and Raquet, J. F.,"Arcjet Cathode Phenomena," presented at the 1989 JANNAF Propulsion Meeting, Cleveland, OH, May 1989 (NASA TM-102099).

25. Curran, F. M., and Haag, T. W.,"Arcjet Component Conditions Through a Multistart Test," AIAA-87-1060, May 1987.

Table I. Arcjet Performance Test Matrix

Mass Flow Rate, kg/s	Thruster Input Power, kW				
	1.00	1.25	1.50	1.75	2.00
3.0×10^{-5}	x	x	a	b	b
4.0×10^{-5}	x	x	x	x	b
5.0×10^{-5}	c	d	x	x	x

x. test points
a. not measured during first performance characterization (0 h)
b. anode housing temperature would have exceeded 1400°C
c. arc voltage would have exceeded 130 Vdc
d. arc voltage would have exceeded 130 Vdc during performance characterization prior to disassembly and inspection

14

Table II. Arcjet Performance Data

Voltage, V	Current, A	Power, kW	Mass Flow Rate, kg/s×10^5	Specific Power, MJ/kg	Thrust, mN	Specific Impulse, s	Efficiency	Feed Pressure, kPa	Housing Temperature, °C
					0 h				
94	10.7	1.00	3.00	33.4	143	485	0.333	392	1127
89	14.0	1.25	3.01	41.5	156	529	0.320	426	1277
109	9.1	0.99	4.00	24.9	173	441	0.366	463	960
103	12.2	1.25	4.03	31.0	191	483	0.354	502	1088
99	15.1	1.50	4.04	37.1	207	523	0.349	533	1222
98	17.9	1.75	4.04	43.4	221	559	0.342	563	1351
121	8.2	0.99	4.99	19.9	197	403	0.381	529	797
113	11.0	1.25	5.00	24.9	221	450	0.381	575	981
109	13.8	1.50	5.00	30.1	241	491	0.377	613	1119
107	16.4	1.75	5.00	35.0	257	524	0.370	643	1225
105	19.0	2.00	5.00	40.0	272	554	0.363	672	1326
					100 h				
104	9.6	1.00	2.99	33.5	143	487	0.335	400	1122
97	12.9	1.26	3.00	41.9	156	530	0.318	435	1249
94	15.9	1.50	3.00	50.1	166	565	0.303	464	1363
121	8.3	1.00	4.01	25.0	176	447	0.376	478	972
111	11.3	1.25	3.98	31.5	193	493	0.365	514	1098
107	14.1	1.51	4.00	37.7	205	522	0.342	550	1239
104	16.7	1.75	4.00	43.6	218	556	0.336	580	1330
123	10.2	1.25	5.02	24.9	224	455	0.391	590	955
118	12.7	1.50	5.03	29.9	244	494	0.385	630	1085
115	15.3	1.75	5.02	34.9	258	524	0.371	664	1206
113	17.7	2.00	5.03	39.8	273	554	0.365	696	1299

Table II (cont'd). Arcjet Performance Data

Voltage, V	Current, A	Power, kW	Mass Flow Rate, kg/s×10^5	Specific Power, MJ/kg	Thrust, mN	Specific Impulse, s	Efficiency	Feed Pressure, kPa	Housing Temperature, °C
				200 h (pre-inspection)					
109	9.2	1.01	2.99	33.6	142	485	0.330	388	1112
102	12.3	1.25	2.99	41.8	155	529	0.317	425	1260
98	15.3	1.50	2.99	50.3	166	566	0.302	456	1389
127	7.9	1.00	4.00	25.0	173	440	0.363	451	953
116	10.8	1.25	4.00	31.3	191	487	0.357	490	1101
111	13.5	1.50	4.00	37.5	207	527	0.350	528	1220
108	16.2	1.75	4.00	43.8	218	557	0.336	566	1328
123	12.2	1.50	5.00	30.0	239	488	0.373	617	1110
119	14.8	1.76	5.02	35.0	256	520	0.365	642	1204
117	17.1	2.00	5.01	39.9	271	550	0.359	672	1305
				200 h (post-inspection)					
99	10.1	1.00	3.00	33.4	143	486	0.333	330	1071
92	13.6	1.25	3.00	41.7	156	531	0.320	356	1204
89	16.8	1.50	3.00	49.9	167	566	0.305	379	1319
119	8.4	1.00	4.00	25.0	173	441	0.366	393	928
108	11.6	1.26	4.01	31.4	193	490	0.360	424	1062
102	14.7	1.50	4.01	37.5	209	532	0.357	451	1178
101	17.4	1.75	4.01	43.6	220	559	0.339	471	1274
122	10.2	1.25	5.02	24.9	221	448	0.379	484	909
113	13.2	1.50	5.02	29.8	241	489	0.378	514	1033
112	15.7	1.76	5.02	34.9	257	522	0.369	542	1153
110	18.3	2.01	5.03	39.9	273	553	0.363	567	1239
108	18.5	2.00	5.02	39.8	274	556	0.367	566	1230

16

anode housing (TZM)

cathode (W/2%ThO2)

rear insulator (BN)

anode (W/2%ThO2)

housing
temperature
location

graphite foil
gasket locations

graphite foil
gasket locations

propellant inlet

plunger (BN)

spring (inconel)

anode/housing
joint

injector disk
(TZM)

front insulator (BN)
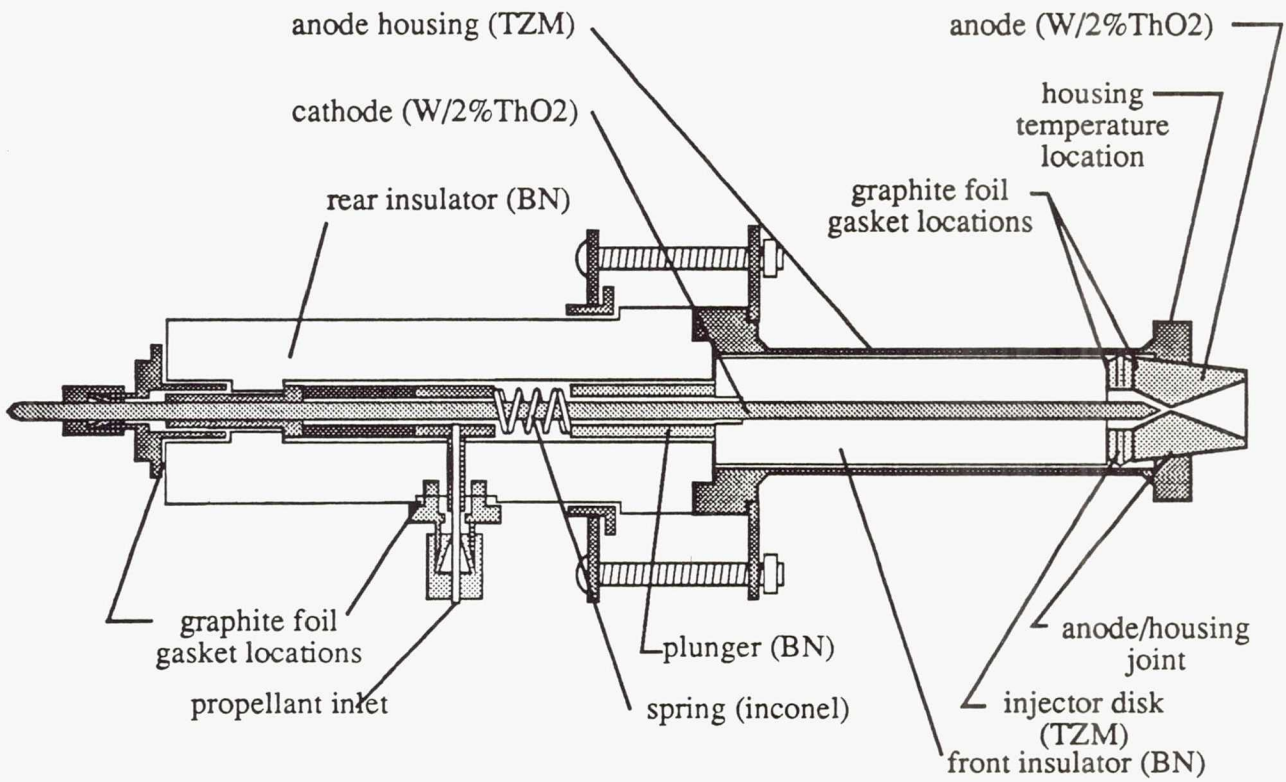
Figure 1. Sectional View of Arcjet Thruster

0.0254 cm

20o

0.055 cm

0.058 cm
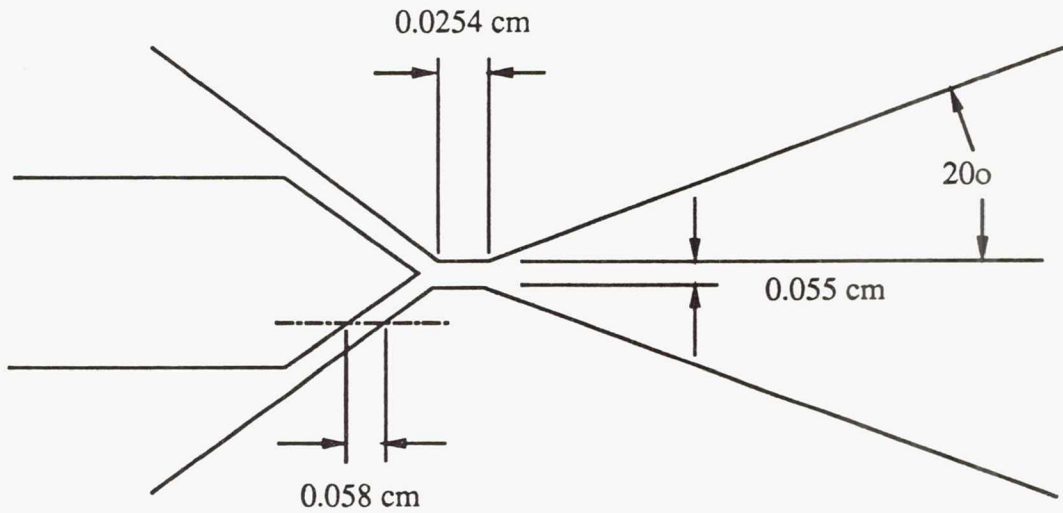
Figure 2. Constrictor Region Detail

17
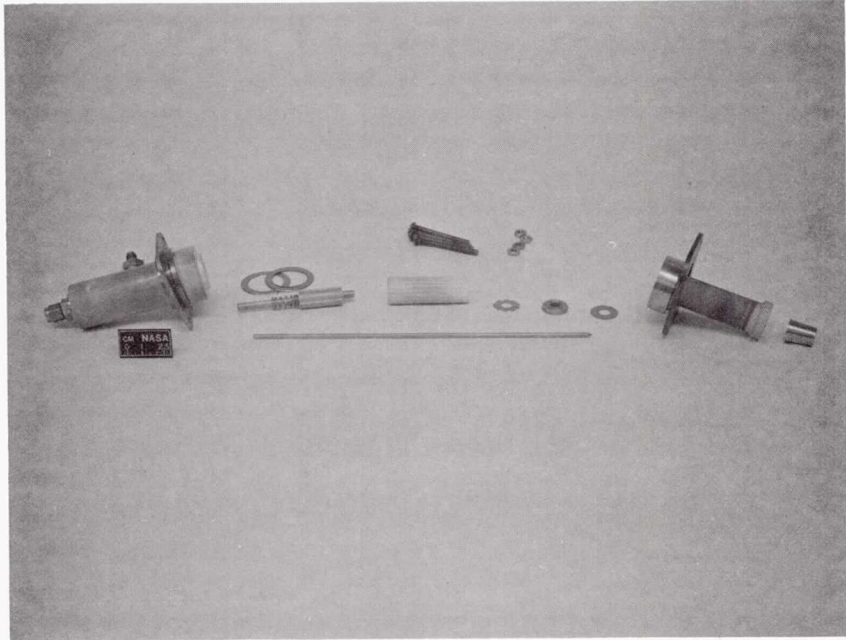
Figure 3. Arcjet Components Prior to Assembly
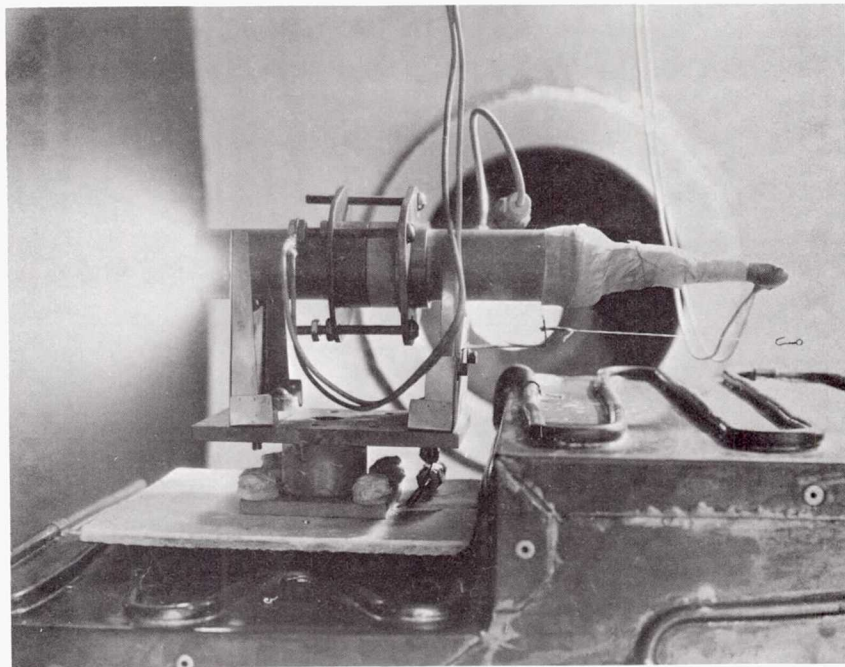
Figure 4. Arcjet Operating in Performance Test Facility
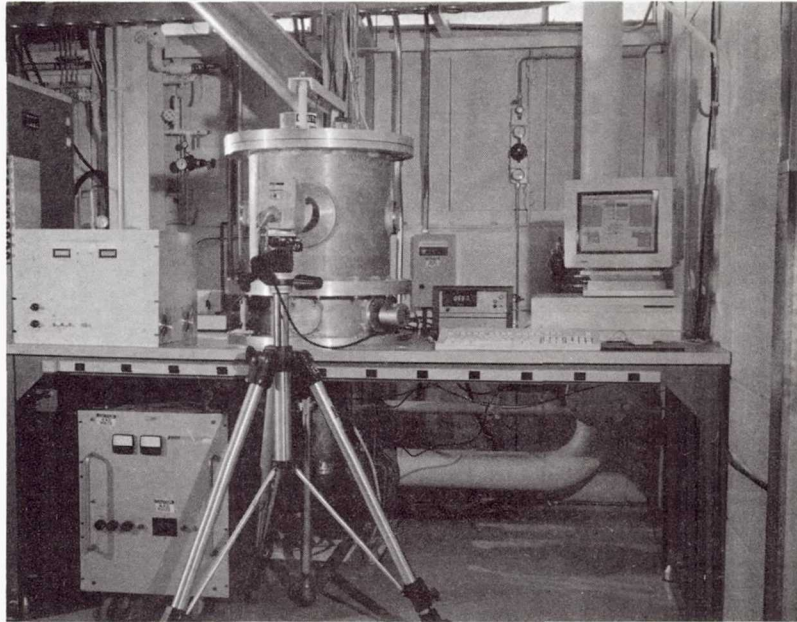
Figure 5. Arcjet Endurance Test Facility
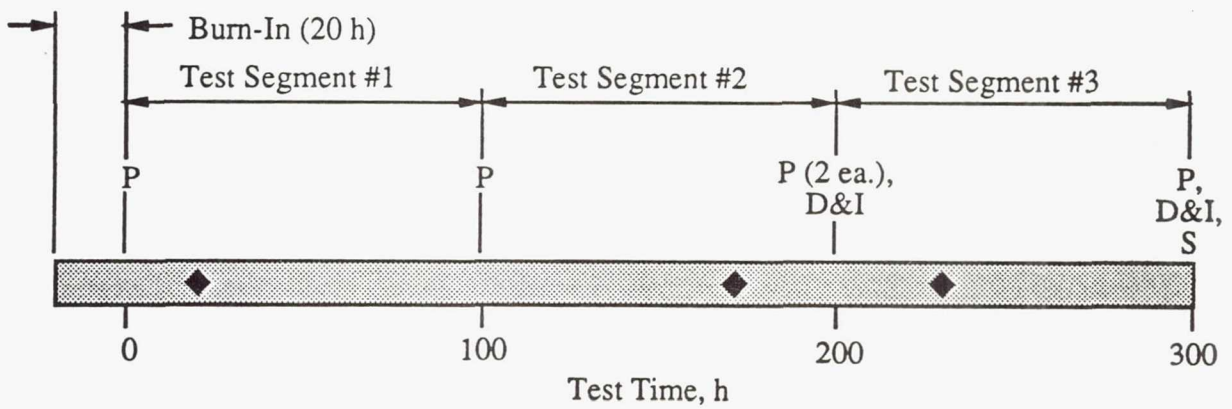
P: Performance Characterization
D&I: Disassembly and Inspection
S: Electrode Sectioning, Analysis
◆ Unintended Shutdown

Figure 6. Test Chronology

19
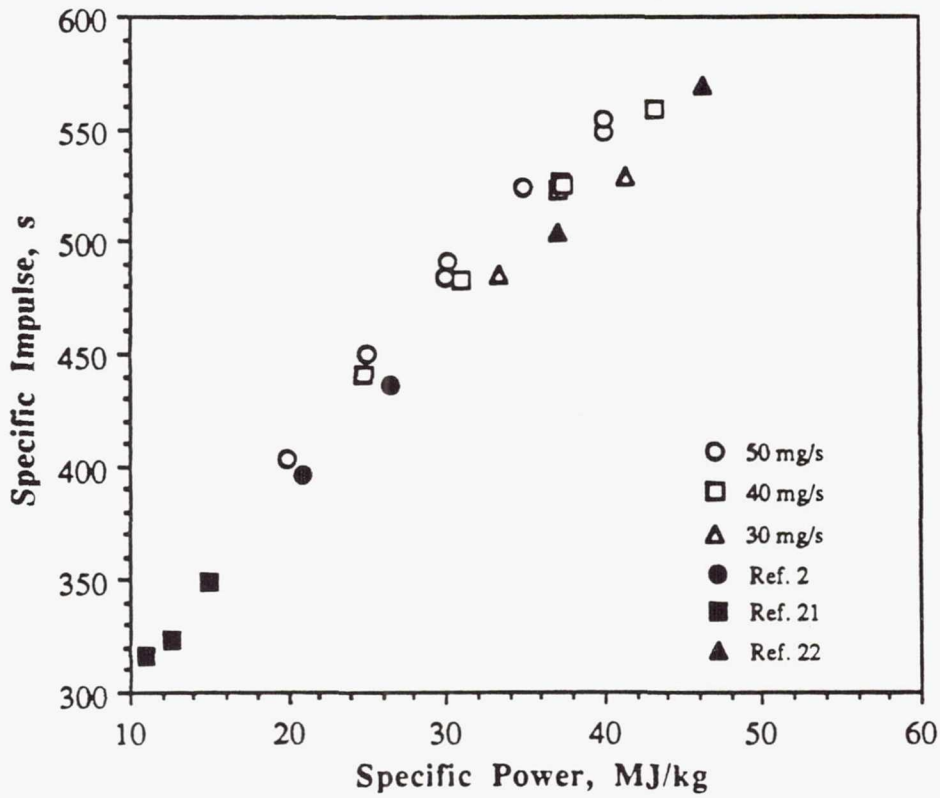
Figure 7. Arcjet Performance Prior to Endurance Test Series
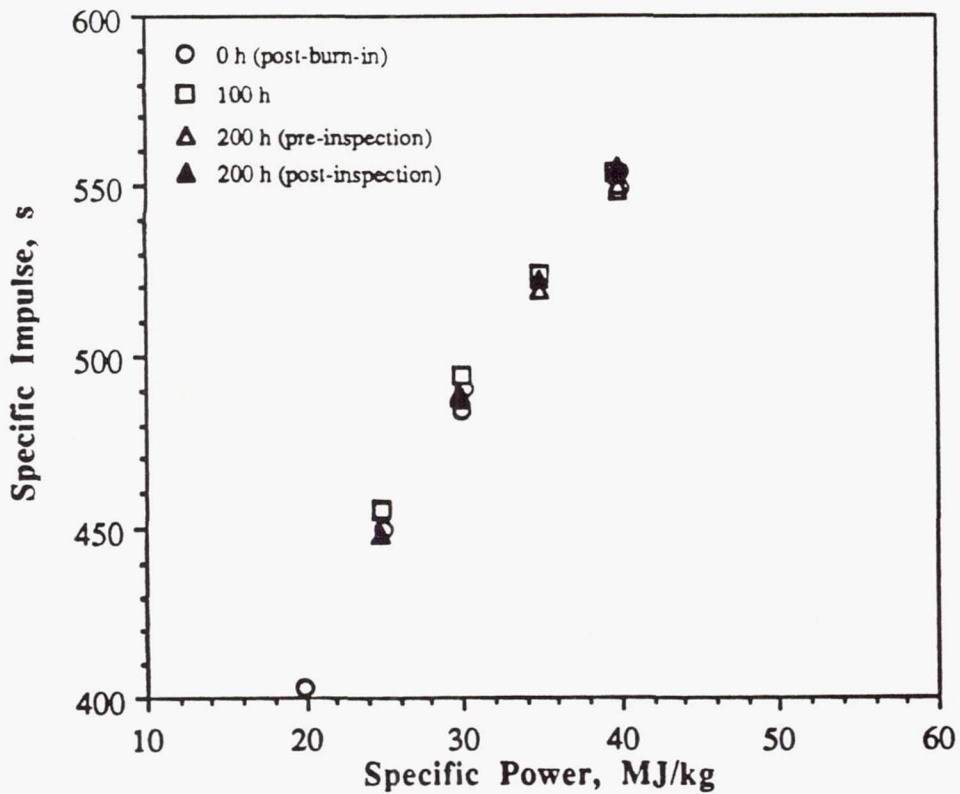
Figure 8. Arcjet Performance During Endurance Test Series
(mass flow rate = 5.0×10^{-5} kg/s)
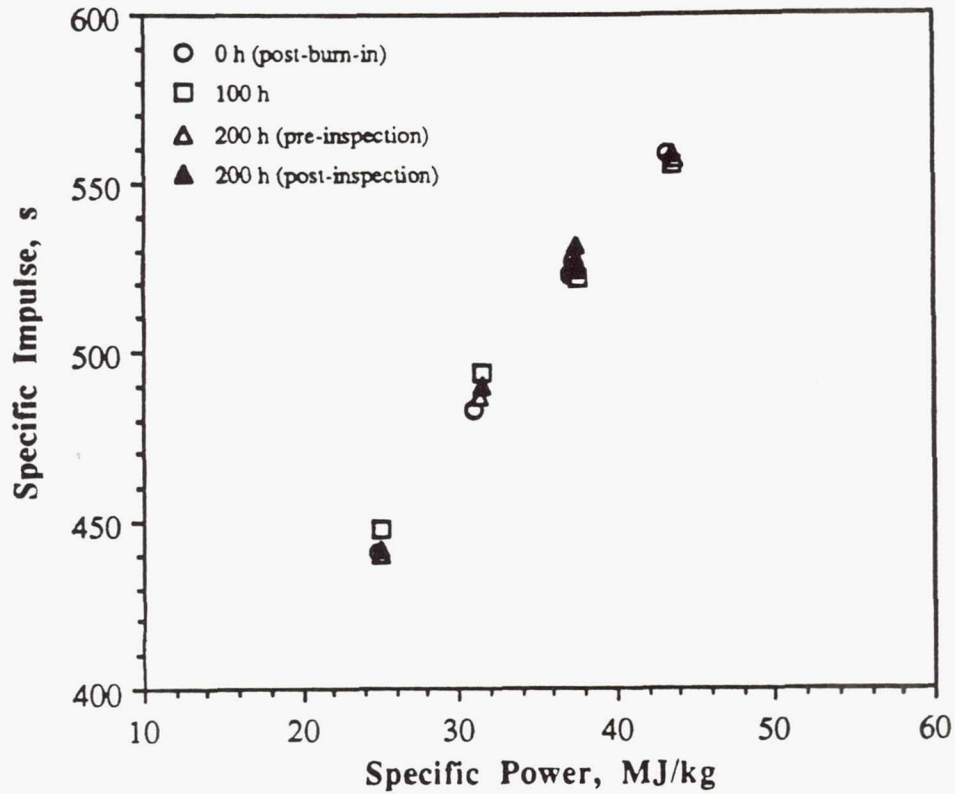
Figure 9. Arcjet Performance During Endurance Test Series
(mass flow rate = 4.0×10^{-5} kg/s)
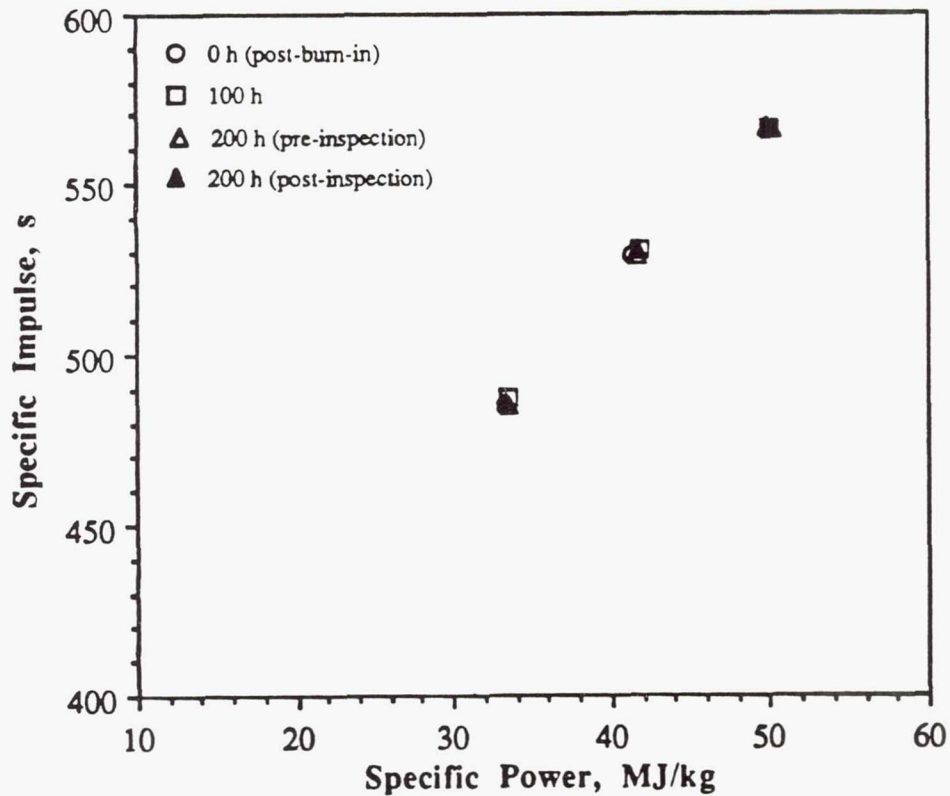
Figure 10. Arcjet Performance During Endurance Test Series
(mass flow rate = 3.0×10^{-5} kg/s)
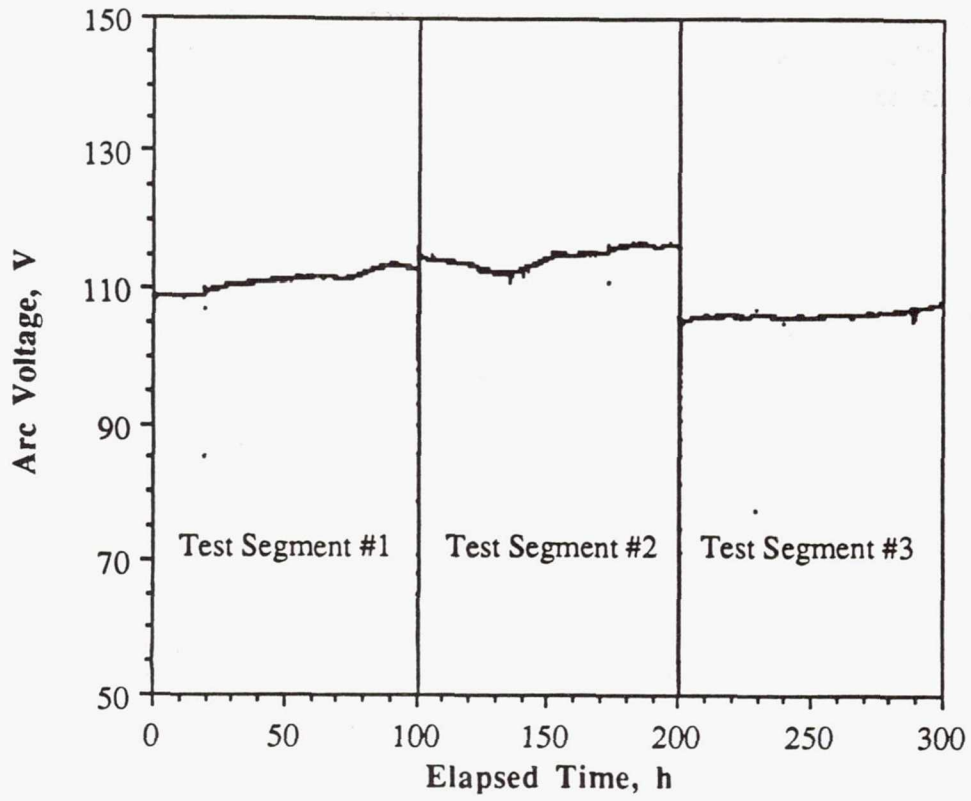
Figure 11. Arc Voltage History
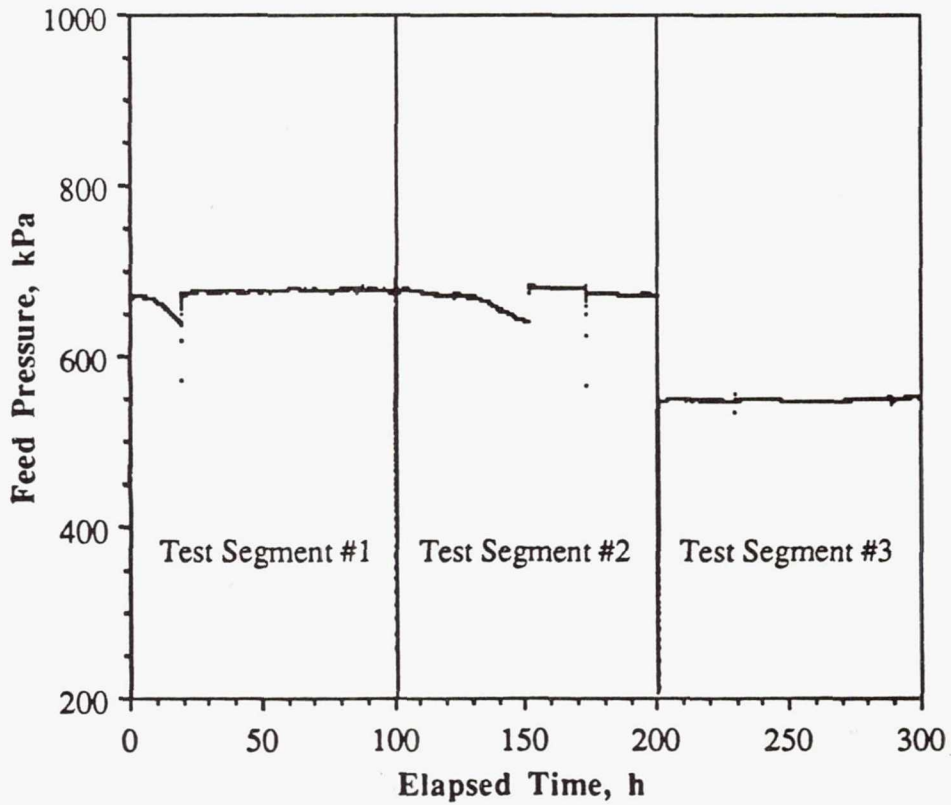
Figure12 Feed Pressure History

22
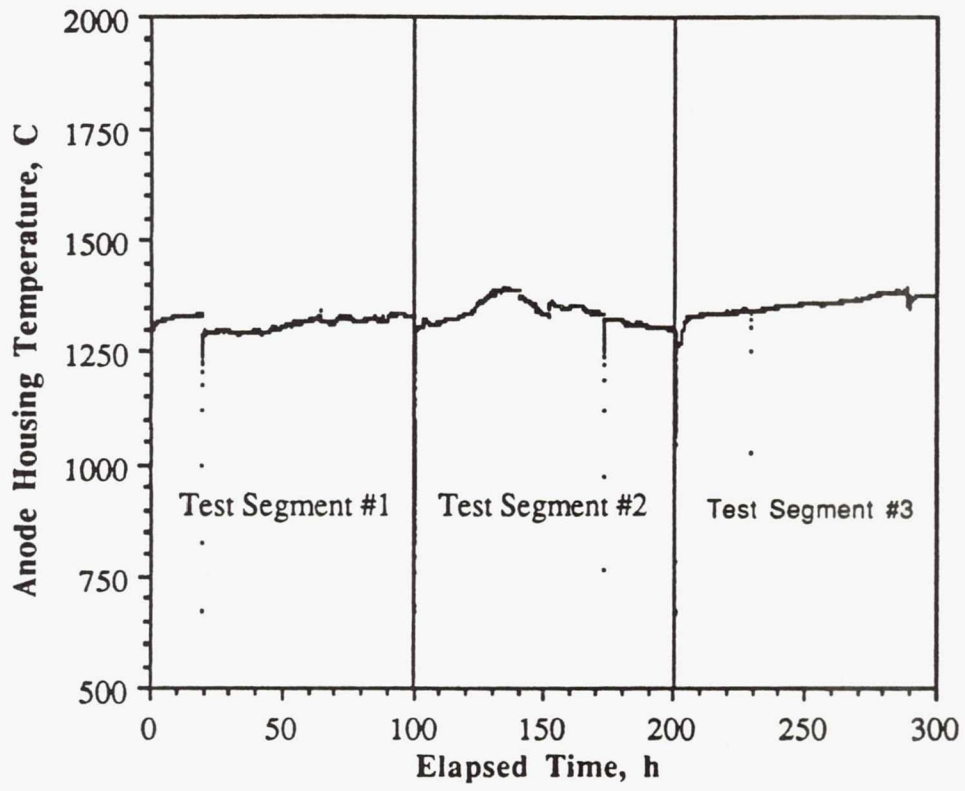
Figure 13. Anode Housing Temperature History
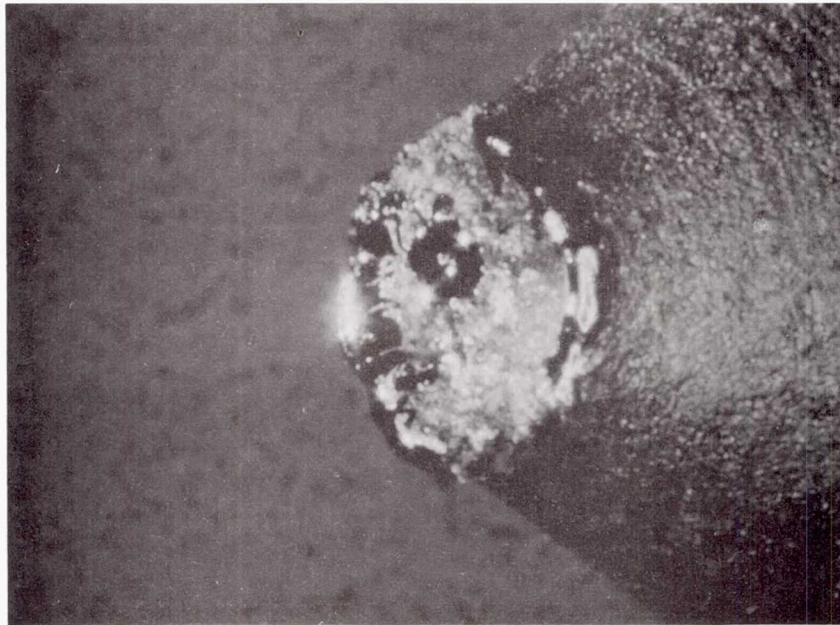
1.0 mm

Figure 14. Cathode Tip After Second 100-h Test Segment
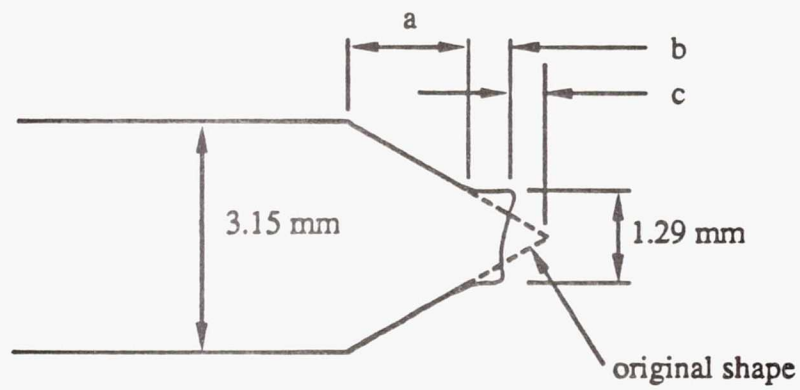
a = 1.60 mm
b = 0.55 mm
c = 0.58 mm

Figure 15. Comparison of Cathode Tip After Second 100-h Test Segment to As-Machined Shape
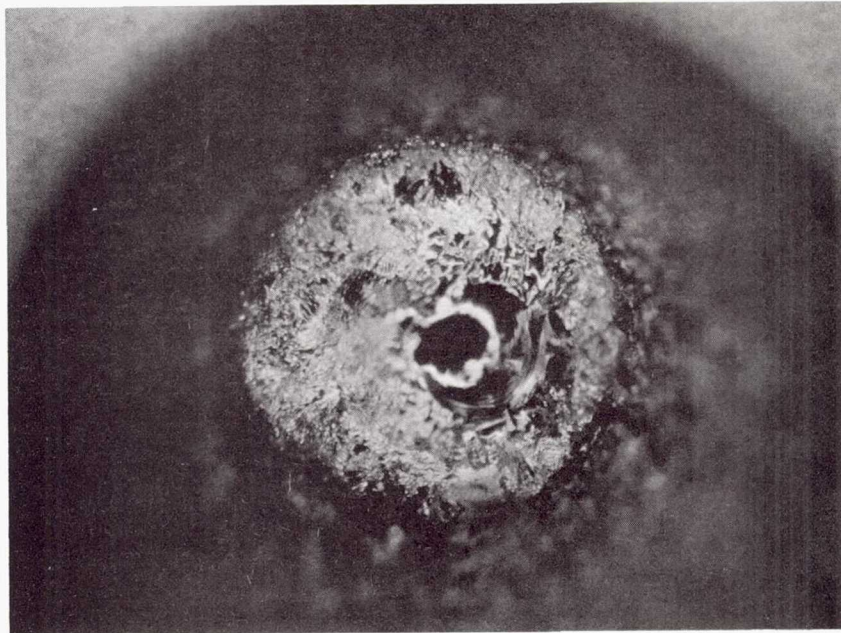
1.0 mm

Figure 16. Cathode Tip After Third 100-h Test Segment
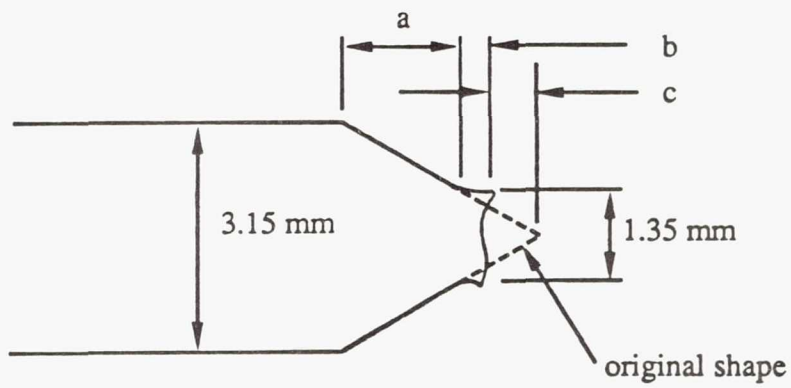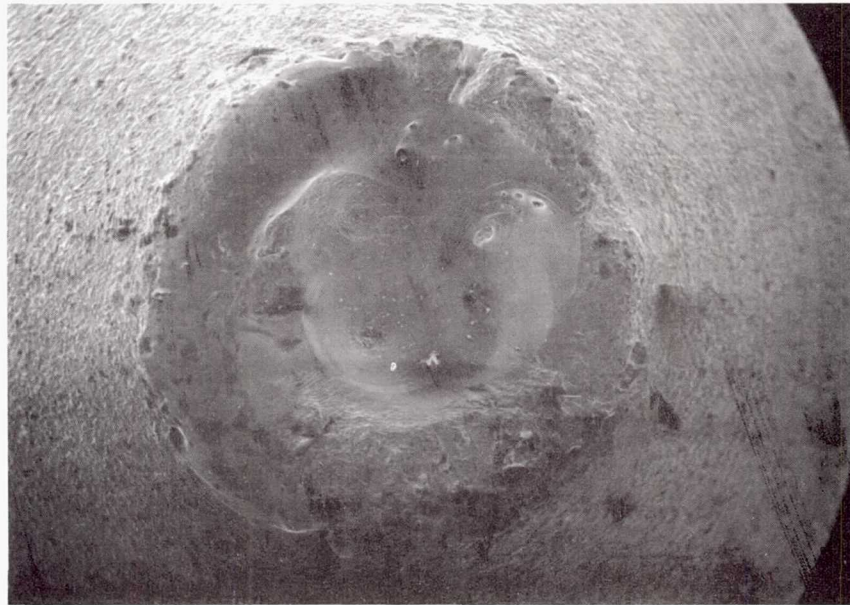

a = 1.56 mm
b = 0.39mm
c = 0.78 mm

**Figure 17. Comparison of Cathode Tip After Second 100-h Test
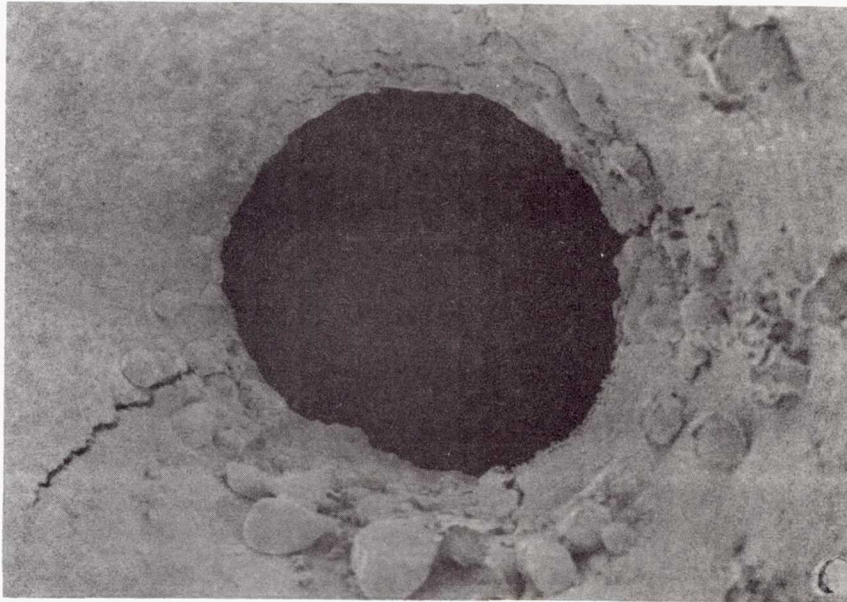Segment to As-Machined Shape**

25
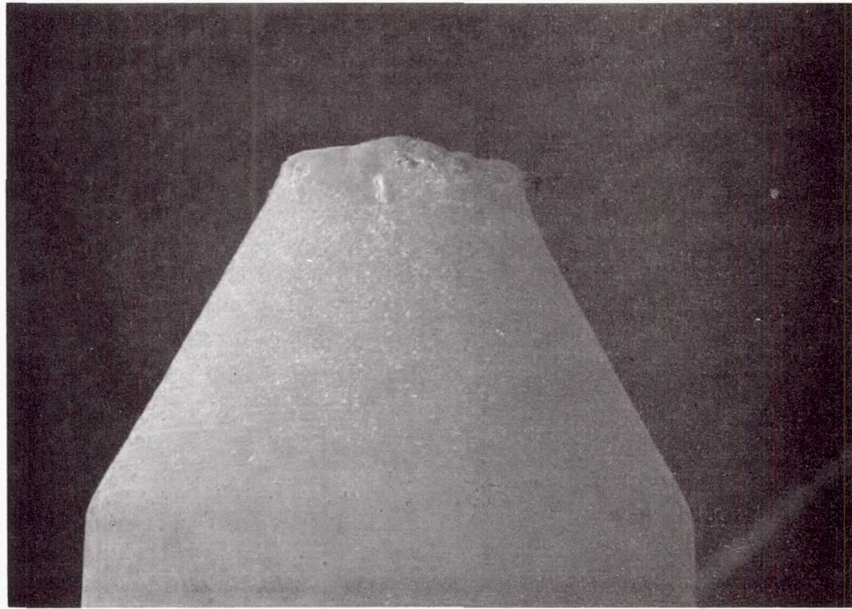
1.0 mm

Figure 18. SEM Photograph of Cathode Tip After Third 100-h
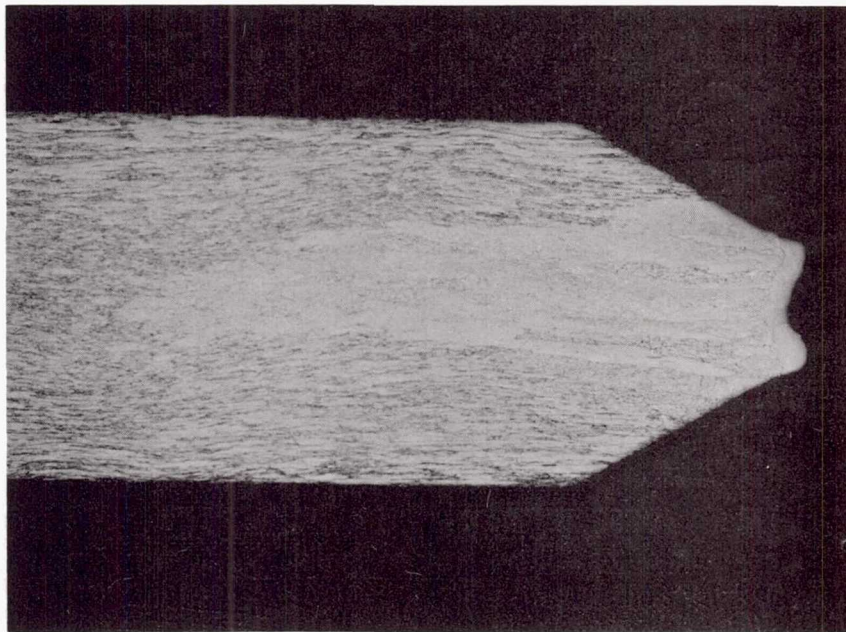Test Segment

0.5 mm

Figure 19. SEM Photograph of Cathode Tip After Third 100-h
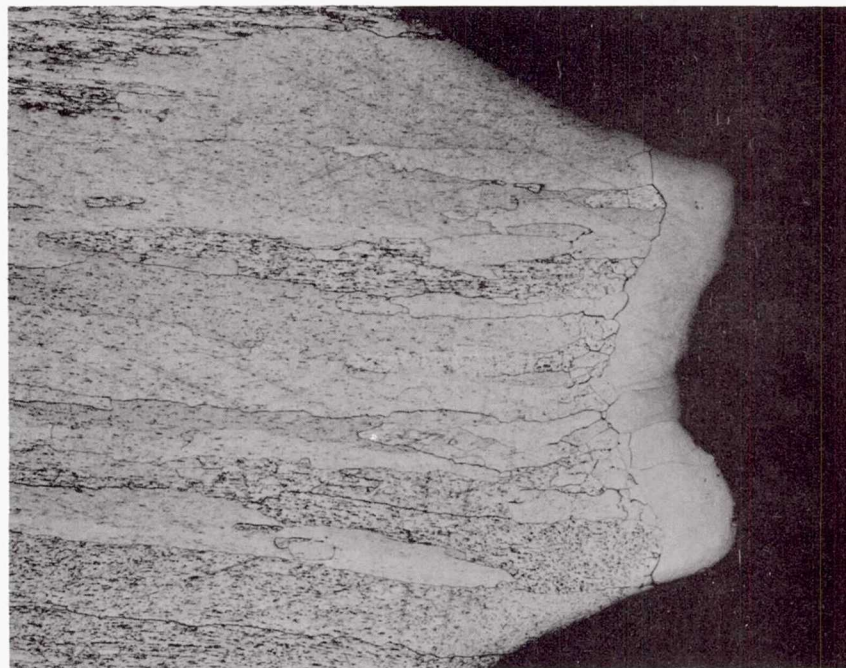Test Segment

26

500 μ m

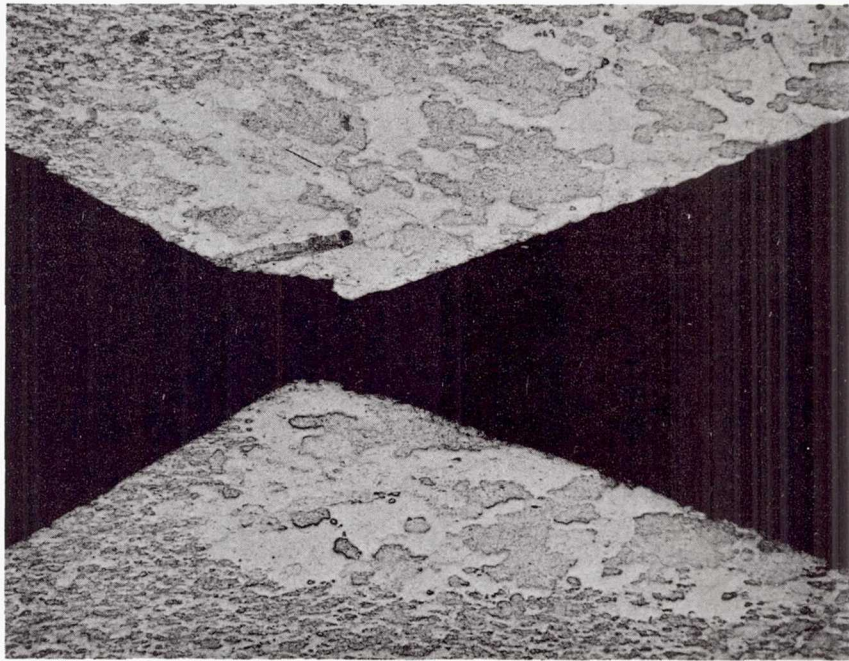**Figure 20. SEM Photograph of Constrictor Exit After Third
100-h Test Segment**

2.0 mm

**Figure 21. Grain Structure of Cathode Tip After Third 100-h
Test Segment**

1.0 mm

**Figure 22. Grain Structure of Cathode Tip After Third 100-h
Test Segment**

28

2.0 mm

**Figure 23. Grain Structure of Constrictor Region After Third
100-h Test Segment**

Report Documentation Page

NASA
National Aeronautics and
Space Administration

1. Report No. NASA TM-105149 AIAA-91-2228	2. Government Accession No.	3. Recipient's Catalog No.

4. Title and Subtitle

Preliminary Performance and Life Evaluations of a 2-kW Arcjet

5. Report Date

6. Performing Organization Code

7. Author(s)

W. Earl Morren and Francis M. Curran

8. Performing Organization Report No.

E-6430

10. Work Unit No.

506-42-31

9. Performing Organization Name and Address

National Aeronautics and Space Administration
Lewis Research Center
Cleveland, Ohio 44135-3191

11. Contract or Grant No.

13. Type of Report and Period Covered

Technical Memorandum

12. Sponsoring Agency Name and Address

National Aeronautics and Space Administration
Washington, D.C. 20546-0001

14. Sponsoring Agency Code

15. Supplementary Notes

Prepared for the 27th Joint Propulsion Conference cosponsored by AIAA, SAE, ASME, and ASEE, Sacramento, California, June 24-27, 1991. Responsible person, W. Earl Morren, (216) 433-2424.

16. Abstract

The first results of a program to expand the operational envelope of low-power arcjets to higher specific impulse and power levels are presented. The performance of a kW-class laboratory model arcjet thruster was characterized at three mass flow rates of a 2:1 mixture of hydrogen and nitrogen at power levels ranging from 1.0 to 2.0 kW. This same thruster was then operated for a total of 300 h at a specific impulse and power level of 550 s and 2.0 kW, respectively, in three continuous 100-h sessions. Thruster operation during the three test segments was stable, and no measurable performance degradation was observed during the test series. Substantial cathode erosion was observed during an inspection following the second 100-h test segment. Most notable was the migration of material from the center of the cathode tip to a ring around a large crater. The anode sustained no significant damage during the endurance test segments. Some difficulty was encountered during start-up after disassembly and inspection following the second 100-h test segment, which caused constrictor erosion. This resulted in a reduced flow restriction and arc chamber pressure, which in turn caused a reduction in the arc impedance.

17. Key Words (Suggested by Author(s))

Electric propulsion
Arc jet engines
Auxiliary propulsion

18. Distribution Statement

Unclassified - Unlimited
Subject Category 20

19. Security Classif. (of the report)	20. Security Classif. (of this page)	21. No. of pages	22. Price*
Unclassified	Unclassified	30	A03

NASA FORM 1626 OCT 86

*For sale by the National Technical Information Service, Springfield, Virginia 22161